Supporting Information

Mn-based tin sulfide $Sr_3MnSn_2S_8$ with wide band gap and strong nonlinear optical response

Chuang Liu,[a] Dajiang Mei,*[a] Wangzhu Cao,[a] Yi Yang,[bc] Yuandong Wu,[a] Guobao Li[d] and Zheshuai Lin*[bc]

[a] College of Chemistry and Chemical Engineering, Shanghai University of Engineering Science, Shanghai 201620, China.
* E-mail: **meidajiang718@pku.edu.cn**
[b] Technical Institute of Physics and Chemistry, Chinese Academy of Sciences, Beijing 100190, China
* E-mail: **zslin@mail.ipc.ac.cn**
[c] University of Chinese Academy of Sciences, Beijing 100190, China
[d] Beijing National Laboratory for Molecular Sciences, State Key Laboratory of Rare Earth Materials Chemistry and Applications, College of Chemistry and Molecular Engineering, Peking University, Beijing 100871, P. R. China

Contents

Experimental sections

Solid-state synthesis

All operations were processed in Ar-protected glove-box. The following purchased reagents, SrS (99.9%), Mn (99.9%), Sn (99.5%), and S (99.99%) were mixed with the molar radio of 3: 1: 2: 5. Next, the mixed reagents were loaded into the graphic crucible. Then, they were put into the silica tube sealed under vacuum ($<10^{-3}$ Pa) and were transferred to the computer-controlled muffle furnace. The temperature program was heated to 1173K in one day, and then there was a 20 hours process of heat preservation. Finally, the sample was cooled to ambient temperature. The Bruker D2 X-ray diffractometer equipped with graphite monochromatized Cu-Kα radiation (λ =1.5418 Å) was used to collect the data of single crystal at room temperature. The 2θ range of X-ray diffraction was from 10° to 70° and 0.02° as a scan step width. The experimental X-ray diffraction data of $Sr_3MnSn_2S_8$ powder was compared with the simulated data in **Figure S1**. And the results showed that the two values are consistent.

Single crystal growth

In an Ar-protected glove-box, the prepared $Sr_3MnSn_2S_8$ powder was mixed with flux KI at the rata of 1: 1 and then the mixtures were loaded into the graphic crucible. Next, the graphic crucible was put into the silica tube and then sealed under vacuum and transferred to a programmed muffle furnace. Afterwards, the program temperature was heated to 1173K in one day and maintain at the current temperature for two days, subsequently, the temperature was cooled to 573K at the slow speed of 2K per hour, and finally, the sample was cooled to ambient temperature. The product was cleaned with deionized water to obtain yellow-green crystals which are stable in air.

Crystal structure determination

The size of single crystal is 0.2mm×0.16mm×0.18mm. The Bruker D8 diffractometer equipped with a graphite-monochromatized Mo-Kα radiation (λ = 0.71073 Å) was used to harvest the single crystal data. The single crystal structure was resolved by the direct method and refined by the full-matrix least squares which is fitted on F^2 by SHELX-2016/6 program package.[1] Structure data and specific details are exhibited in **Table S1**.

Diffuse reflectance spectroscopy analysis

The UV−vis−NIR diffuse reflectance spectroscopy data of $Sr_3MnSn_2S_8$ was tested by the Shimadzu UV-3600 spectrophotometer within the range from 200nm to 1500nm.

Laser Damage Threshold Test

A pulsed YAG laser (1.06 μm, 10 ns, 10 Hz) was used to carry out the laser damage threshold test, meanwhile, an $AgGaS_2$ sample with similar size was provided as a reference material.

Second Harmonic Generation Measurement

The second harmonic generation test was carried out by Kurtz-Perry[2] method with the laser of 1.06 μm Q-switched Nd: YAG. $AgGaS_2$ as a reference material which is the same particle size have been used. The

particle size of the test sample was 70-90 μm, and the $AgGaS_2$ used for reference had the same particle size.

Computational method

The spin-polarized first-principle calculations for compound $Sr_3MnSn_2S_8$ was performed by CASTEP,[3] which is a total energy package of plane-wave pseudopotential according to density functional theory (DFT).[4] The exchange-correlation energy was depicted by the local density approximation (LDA)[5,6] which was exploited by Ceperley, Alder, Perdew, and Zunger (CA-PZ). The optimized norm-conserving pseudopotentials[7] in the Kleinman-Bylander[8] form wist respect to all the elements in compound $Sr_3MnSn_2S_8$ were used to simulate the effective interaction between valence electrons and atom cores, without decreasing the computational accuracy, a relatively small basis set was allowed to adopt. Sr $4s^24p^65s^2$ Mn $3d^54s^2$ Sn $5s^25p^2$ and S $3s^23p^4$. A high cutoff energy with 800 eV was selected. Moreover, in order to describe the localized d-orbitals in Mn atoms, the LDA + U method[9,10] was adopted by setting the on-site orbital dependent Hubbard U energy as Ud = 2.5eV.

Table S1. Crystallographic data and refinement details of $Sr_3MnSn_2S_8$

	$Sr_3MnSn_2S_8$
Fw	811.66
a (Å)	14.2287(6)
b (Å)	14.2287(6)
c (Å)	14.2287(6)
Volume ($Å^3$)	2880.7(4)
Space group	$I\bar{4}3d$
Z	8
Index ranges	$-16 \leq h \leq 16$
	$-16 \leq k \leq 16$
	$-16 \leq l \leq 16$
ρ_c (Mg m^{-3})	3.743
μ (mm^{-1})	16.412
$R(F)$[a]	0.0104
$R_w(F_o^2)$[b]	0.0247
Weight = 1 / [sigma^2(F_o^2) + (0.0220 * P) ^2 + 84.95 * P]	
where P = (Max (Fo^2, 0) + 2 * F_c^2) / 3	

Table S2. Selected bond lengths (Å) and angles (deg) of $Sr_3MnSn_2S_8$

Sr-S1×2	3.0247(7)
Sr-S2×2	3.0966(11)
Sr-S2×2	3.1480(10)
Sr-S2×2	3.3644(12)
Mn-S2×4	2.4761(10)
Sn-S1×1	2.3437(18)
Sn-S2×3	2.3986(11)
S1-Sn-S2×3	112.53(3)
S2-Sn-S2×3	106.25(3)
S2-Mn-S2×4	95.359(13)
S2-Mn-S2×2	144.41(4)

Table S3. SHG responses and band gaps of Sn-containing compounds

Compounds	Band gaps (eV)	SHG responses	Ref.
$Na_2Ba_7Sn_4S_{16}$	2.50	0.1× AGS	11
$Na_2Ba_7Sn_4Se_{16}$	2.10	0.2× AGS	11
$Li_2Ba_7Sn_4S_{16}$	2.30	0.5× AGS	11
$Li_2Ba_7Sn_4Se_{16}$	1.75	0.4× AGS	11
$Ba_7Sn_5S_{15}$	2.29	2× AGS	12
$Ba_8Sn_4S_{15}$	2.31	10× AGS	13
$BaAg_2SnS_4$	1.77	0.4× AGS	14
$Sr_3MnSn_2S_8$	2.33	~AGS	This work

Figure S1. The experimental and simulated X-ray diffraction result of $Sr_3MnSn_2S_8$ powder

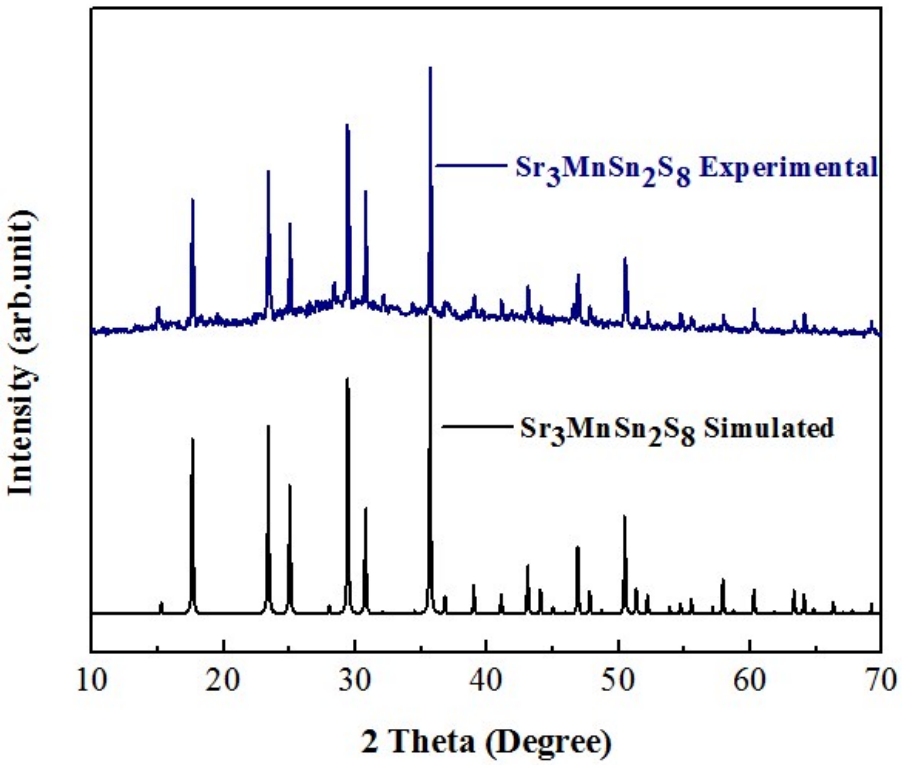

Figure S2. Diffuse spectrum of $AgGaS_2$ using upper tangent method

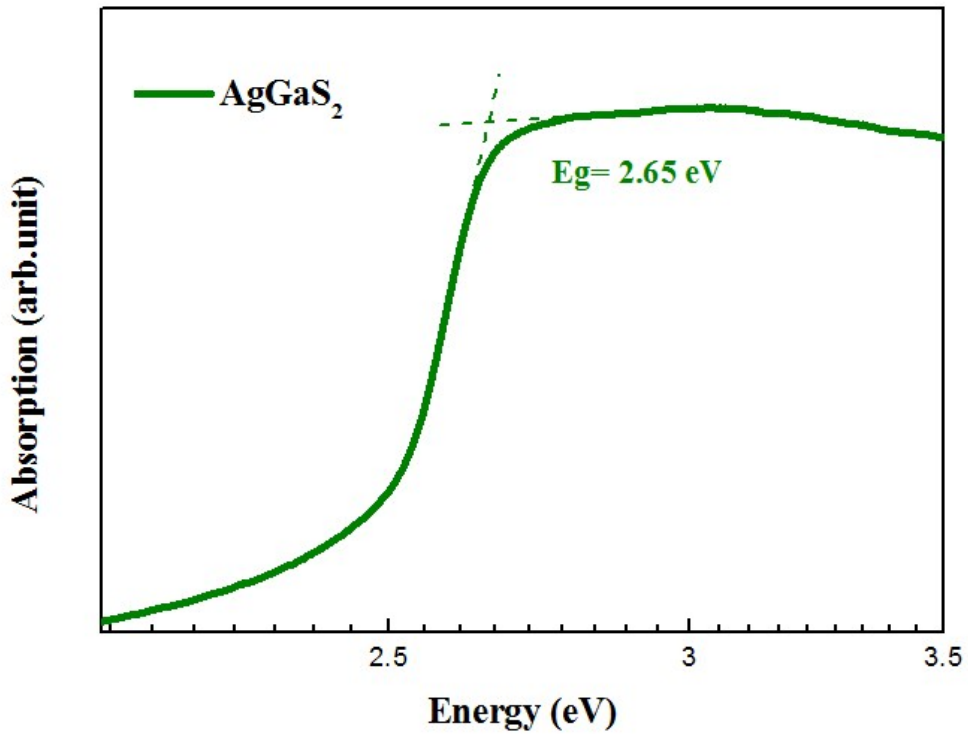

Figure S3. Diffuse spectrum of $Sr_3MnSn_2S_8$ using baseline tangent method

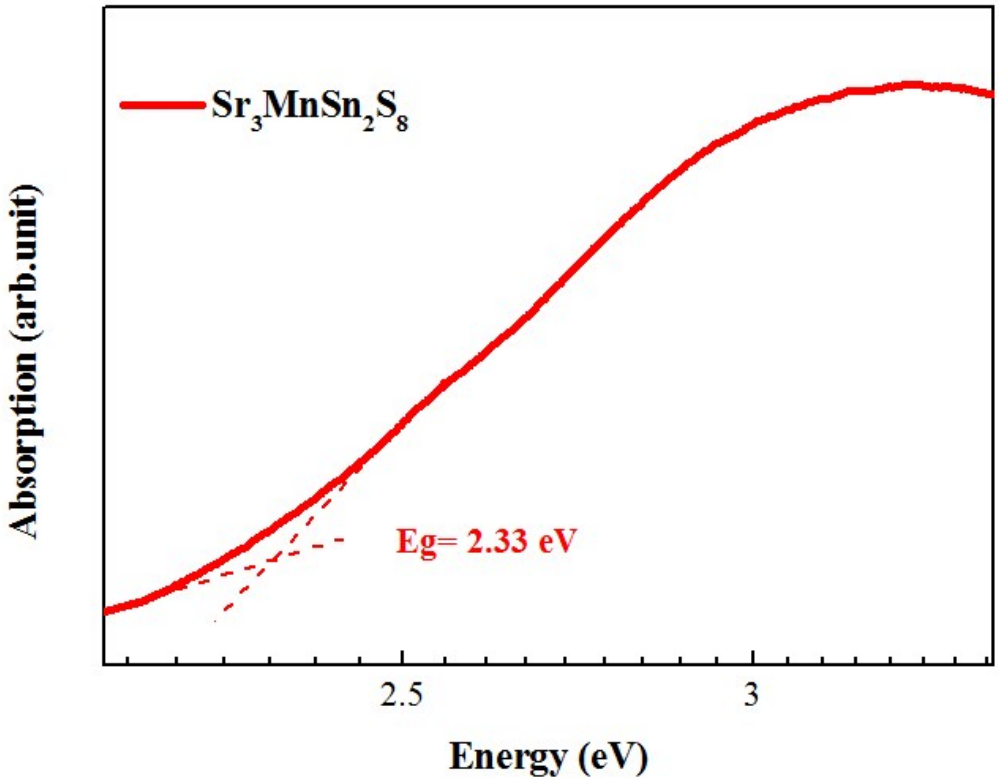

References

1. G. M. Sheldrick, *Acta Cryst.*, 2015, **71**, 3-8.
2. S. K. Kurtz and T. T. Perry, *J. Appl. Phys.*, 1968, **39**, 3798-3813.
3. S. J. Clark, M. D. Segall, C. J. Pickard, P. J. Hasnip, M. I. J. Probert, K. Refson and M. C. Payne, *Z. Kri.*, 2005, **220**, 567-570.
4. M. C. Payne, M. P. Teter, D. C. Ailan, T. A. Arias and J. D. Joannopouios, *Rev. Mod. Phys.*, 1992, **64**, 1045-1097.
5. D. M. Ceperley and B. J. Alder, *Phys. Rev. Lett.*, 1980, **45**, 566-569.
6. J. P. Perdew and A. Zunger, *Phys. Rev. B*, 1981, **23**, 5048-5079.
7. A. M. Rappe, K. M. Rabe, E. Kaxiras and J. D. Joannopoulos, *Phys. Rev. B*, 1990, **41**, 1227-1230.
8. L. Kleinman and D. M. Bylander, *Phys. Rev. Lett.*, 1982, **48**, 1425-1428.
9. A. Roldán, M. Boronat, A. Corma and F. Illas, *J. Phys. Chem. C*, 2010, **114**, 6511-6517.
10. F. H. ElBatal, Y. M. Hamdy and S. Y. Marzouk, *J. Non-Cryst. Solids*, 2009, **355**, 2439-2447.
11. A. Abudurusuli, K. Wu and S.-L. Pan, *New J. Chem.*, 2018, **42**, 3350-3355.
12. Z.-Z. Luo, C.-S. Lin, W.-D. Cheng, H. Zhang, W.-L. Zhang and Z.-Z. He, *Inorg. Chem.*, 2013, **52**, 273-279.
13. Z.-Z. Luo, C.-S. Lin, W.-L. Zhang, H. Zhang, Z.-Z. He and W.-D. Cheng, *Chem. Mater.*, 2014, **26**, 1093-1099.
14. H. Chen, P.-F. Liu, B.-X. Li, H. Lin, L.-M. Wu and X.-T. Wu, *Dalton Trans.*, 2018, **47**, 429-437.